Int. J. Heat Mass Transfer. Vol. 21, pp. 1143–1156

0017-9310/78/0801-1143

AN INVESTIGATION OF HEAT TRANSFER AND FRICTION FOR RIB-ROUGHENED SURFACES

J. C. HAN, L. R. GLICKSMAN and W. M. ROHSENOW
Department of Mechanical Engineering, Massachusetts Institute of Technology, Cambridge, MA 02139, U.S.A.

(*Received* 23 *August and in revised form* 6 *February* 1978)

Abstract—An investigation of rib-roughened surface was undertaken to determine the effects of rib shape, angle of attack and pitch to height ratio on friction factor and heat-transfer results. A parallel plate geometry was used. Based on the law of the wall similarity and the application of the heat-momentum analogy developed by Dipprey and Sabersky, a general correlation for friction factor and heat transfer was developed to account for rib shape, spacing and angle of attack. Ribs at a 45° angle of attack were found to have superior heat transfer performance at a given friction power when compared to ribs at a 90° angle of attack or when compared to sand-grain roughness.

NOMENCLATURE

A, surface area;
c_p, specific heat of air;
D_h, hydraulic diameter;
e, rib height;
e^+, $(e/D_n)Re(f/2)^{1/2}$ roughness Reynolds number;
f, friction factor, see equation (1);
G, ρU_m, flow rate;
h, heat-transfer coefficient;
H_e^+, heat-transfer function, see equation (14);
L, test section length;
$\dot{m}$, mass flow rate;
Nu, Nusselt number;
ΔP, pressure drop;
Pr, Prandtl number;
p, rib pitch;
$\dot{q}$, heat-transfer rate;
R, tube radius;
R_e^+, roughness function, see equation (6);
Re, Reynolds number;
St, Stanton number;
T, temperature;
T_f, bulk mean air temperature;
T_m, average air temperature;
T_w, temperature at the wall;
U, local velocity at the X-direction;
U_c, velocity at the centerline;
U_m, average velocity in the X-direction;
U^*, friction velocity, $(\tau_0/\rho)^{1/2}$;
U^+, dimensionless velocity, $\bar{U}/U^*$;
w, rib width;
y, distance from the wall;
y_0, distance to centerline;
y_m, distance from the wall where $T = T_m$, $U = U_m$;
y^+, dimensionless length, $(y/D_h)Re(f/2)^{1/2}$.

Greek symbols

α, flow attack angle;
α, thermal diffusivity;
ε_h, eddy diffusivity for heat transfer;
ε_m, eddy diffusivity for momentum transfer;
ν, kinematic viscosity;
ρ, average air density;
τ_0, shear stress acting on the wall;
ϕ, rib shape angle.

Subscripts

s, smooth surface.

1. INTRODUCTION

A WELL-KNOWN method to increase the heat transfer from a surface is to roughen the surface either randomly with a sand grain or by use of regular geometric roughness elements on the surface. However, the increase in heat transfer is accompanied by an increase in the resistance to fluid flow. Many investigators have studied this problem in an attempt to develop accurate predictions of the behavior of a given roughness geometry and to define a geometry which gives the best heat-transfer performance for a given flow friction.

An early study of the effect of roughness on friction and the velocity distribution, was performed in 1933 by Nikuradse [1] who conducted a series of experiments with pipes roughened by sand grains. One of the first studies of heat transfer in rough tubes was conducted in 1941 by Cope [2], and a very thorough study largely involving two dimensional roughness elements by Nunner [3] in 1958. A number of friction and heat-transfer measurements have been performed for repeated-rib roughness in tube flow, such as Sams [4] in 1952, Broullette [5] in 1957, Koch [6] in 1960, Gargaud and Paumard [7] in 1964, Molloy [8] in 1967 and Kalinin [9] in 1967. Webb, Eckert and Goldstein [10] performed experiments on a tube with internal ribs. The data of Webb *et al.* covered a wide range of rib height to hydraulic diameter ratio, but only a pitch to height ratio greater than ten was used, and the ribs were aligned normal to the main stream direction.

In the nuclear reactor area, considerable data exists for repeated-rib roughness in an annular flow geo-

metry in which the inner annular surface is rough and the outer surface is smooth, such as data reported by Wilkie [11] in 1966, and Sheriff and Gumley [12] in 1966. When both surfaces are smooth, the annular flow friction data can be correlated by the hydraulic diameter, but the concept does not hold when only one surface of the annulus is roughened. Hall [13] proposed that when data taken for an annulus with one rough wall and one smooth wall was based on an equivalent diameter, it should agree with the results obtained in pipe flow for a geometrically similar roughness. Wilkie using a simplification to the Hall transformation, found that a surface has the highest Stanton number and friction factor when the pitch to height ratio is between seven and eight. White and Wilkie [14] studied the heat transfer and pressure loss characteristics of a rib roughened surface with different helix angles. They found that a 33° helix angle with a rib pitch to height ratio of eight showed the greatest gain in performance over that of a zero helix angle (i.e. a traverse rib). However, for the same geometrically similar roughness and flow condition, Wilkie's data does not agree with the measurements of Webb *et al.* Recently, Dalle Donne and Meyer [15] have pointed out a number of drawbacks to the transformation method Wilkie used. Various modifications have been proposed to the original methods to transform the rough surface data taken with annular geometry to a form useful for a simple channel. A resolution of the conflicting results reached by the various transformations must be made before the data taken for the annular geometry can be used with complete confidence.

Thus, although turbulent heat transfer and friction in tubes or annulii with repeated-rib rougheners has been investigated extensively, a number of discrepancies appear in the results and some parameters have not been carefully explored. Specifically, most of the investigators have concentrated on high Reynolds number flow, about 10^5–10^6, with a small ratio of rib height to hydraulic diameter, between 10^{-2} and 10^{-3}. For turbulent flows at lower Reynolds numbers a larger rib height to hydraulic diameter ratio is needed to achieve fully rough flow conditions. Dalle Donne and Meyer [15] have proposed a new correlation for roughened surfaces which indicates a rather significant influence due to the rib height-to-hydraulic diameter ratio. Since the correlation is based on data taken in an annulus which required a transformation to an equivalent hydraulic diameter, a verification is needed using a test geometry which does not require a transformation to reduce the data to a standard form. In addition, when the rib height to hydraulic diameter ratio is large, the relative position of one ribbed surface to an adjacent ribbed surface, Fig. 1, may influence the results.

For ribs perpendicular to the main flow, the rib will induce the largest form drag. As the angle of attack decreases below ninety degrees, the form drag should decrease substantially and the results of Wilkie suggest that a better thermal to hydraulic performance can be obtained. Establishment of the optimum angle of attack is important.

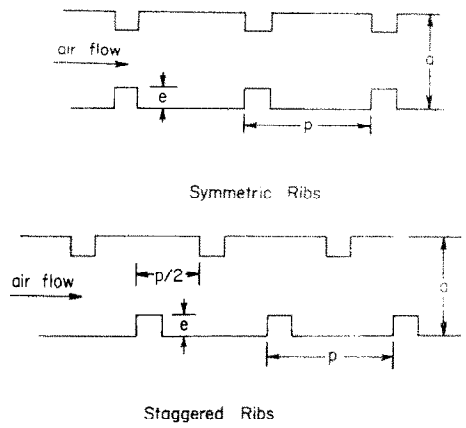

FIG. 1. Symmetric and staggered ribs.

Finally, in many applications, ribs cannot be made to have a square cross-section. The influence of the rib profile on the rib performance should be established.

A study of the influence of above parameters on the performance of repeated rib rougheners was recently completed. This paper will first describe the experimental results. The results will then be compared with previous investigators and a general correlation for the friction factor and the heat-transfer coefficient will be presented.

II. APPARATUS

A parallel plate test section with two identical plates was chosen for two reasons: to eliminate the need of a procedure such as the Hall transformation for data reduction and generalization and to simplify the construction of the various rib geometries.

Figure 2 shows a schematic drawing of the experimental apparatus. A blower forced air at room temperature and pressure through a 10.16 cm (4 in) diameter tube equipped with an ASME square-edge orifice plate to measure flow rates. A long transition section was used between the pipe and the rectangular cross-section to insure that the air entering the test section had a uniform velocity distribution. At the end of the test section, the air was exhausted into the atmosphere. Figure 3 shows the test section which consists of two heated parallel aluminum plates of identical geometry. The plates were 0.635 cm ($\frac{1}{4}$ in) thick to reduce the axial heat conduction to a negligible level, 152 cm (60 in) long so that the thermal and hydraulic profiles were fully developed in the last half of the test section, and 30.5 cm (12 in) wide so that the opposing plates give results approaching that for a pair of infinite parallel plates. The distance between opposing plates was between 2.5 cm (1 in) and 1.3 cm ($\frac{1}{2}$ in) for all tests. The opposing plates were clamped tightly between continuous metal spacers to assure that the distance between the plates remained constant. Woven heaters embedded in silicone rubber were clamped uniformly between a wood panel and the aluminum plate to

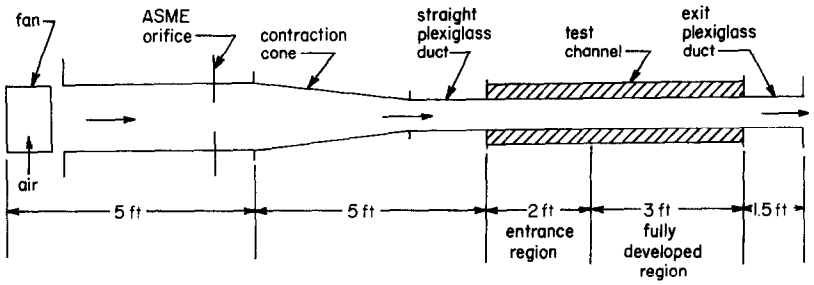

FIG. 2. Top view of the experimental apparatus.

insure good contact. The heaters provided a constant heat flux for the entire test surface. Each aluminum plate had four woven heaters; each heater could be independently controlled. The blower was capable of providing a range of air velocities so that the Reynolds number based on the hydraulic diameter could be varied between 3000 and 30 000. The pressure drop

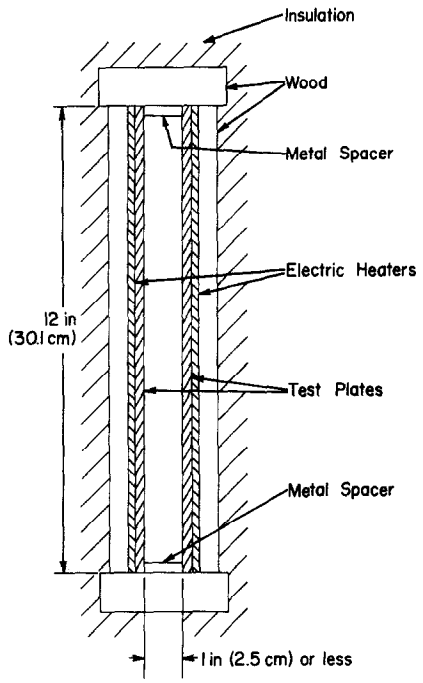

FIG. 3. Cross-section of test section.

across the test section was measured by a micromanometer and an inclined manometer. Nineteen thermocouples were placed on each plate, see Fig. 4. Both plates had identical thermocouple locations to assure symmetry. Thermocouples were also used to measure the bulk mean air temperature entering and leaving the test section. In all tests, in order to reduce the thermocouple inaccuracy which strongly affects the calculated heat transfer coefficient the temperature rise of air was maintained between 22 and 33°C (40 and 50°F) and the temperature difference between the wall and fluid was maintained between 17 and 22°C (30 and 40°F).

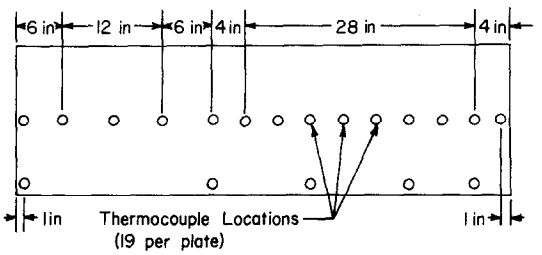

FIG. 4. Detail of thermocouple locations on test plates.

III. EXPERIMENTAL ACCURACY

In fully developed channel flow, the friction factor can be determined by measuring the pressure drop across the flow channel and measuring the mass flow rate of the air. With this data, the friction factor can be calculated from its definition.

$$f = \frac{\Delta P}{4(L/D_h)(G^2/2\rho g_c)}. \quad (1)$$

The maximum uncertainty in the friction factor was estimated to be 6.1%. The Stanton number can be calculated from:

$$St = \frac{\dot{q}}{Gc_p A_s(T_w - T_f)}. \quad (2)$$

The heat-transfer rate can be found from the energy dissipated by the heater or from the energy rise of the air. Both were calculated and compared for all experimental data. The maximum uncertainty in the Stanton number was estimated to be 5.8%.

Before initiating experiments with rib-roughened surfaces, the friction factor and heat-transfer coefficient were measured for smooth plates and compared with the results given in the literature for turbulent flow through smooth walled tubes. Pressure drop measurements were performed without heat addition to the test section. The static pressure distribution was measured by using seven pressure taps along the top flow channel. The results of friction factor and Stanton number for the smooth plates are shown in Fig. 5. As seen by the figure there is good agreement between the accepted correlation [16] and the experimental results for the smooth plate case. The friction factor differs about 6% from tube flow results, and the Stanton number differs by about 5%. The behavior of the friction factor agrees with the data compiled by

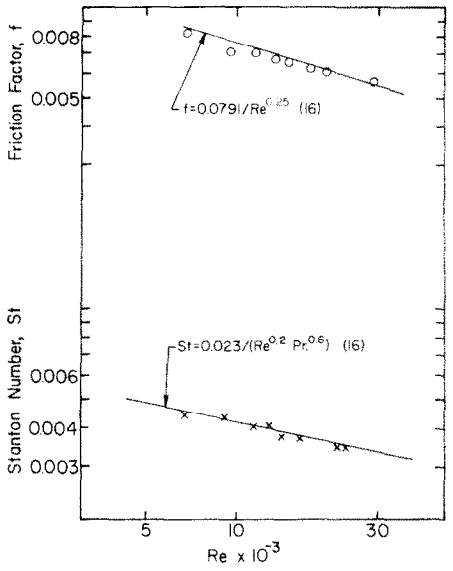

FIG. 5. Test results for smooth surfaces.

Hartnett *et al.* [17] who found that the experimental friction factors for rectangular ducts at Reynolds numbers of 10^4 and below generally fall slightly below the circular tube results.

IV. EXPERIMENTAL RESULTS

The apparatus was used in a series of tests on rib-roughened plates. Sixteen different geometries were tested. They are listed in Table 1. In the tests the

Table 1. Rib geometries tested

p/e	e/D_h	α	ϕ	e/w
5	0.076	90°	90°	1.0
5	0.056	90°	90°	1.0
5	0.046	90°	90°	1.0
5	0.046	90°	55°	1.0
5	0.046	90°	40°	1.0
7.5	0.056	90°	90°	0.67
7.5	0.042	90°	90°	0.67
7.5	0.032	90°	90°	0.67
15	0.056	90°	90°	0.67
15	0.032	90°	90°	0.67
10	0.102	90°	90°	1.0
10	0.102	45°	90°	1.0
10	0.102	20°	90°	1.0
20	0.102	75°	90°	1.0
20	0.102	45°	90°	1.0
20	0.102	20°	90°	1.0

following parameters were systematically varied: the rib height-to-hydraulic diameter, the rib spacings-to-rib height, the rib profile, and the angle of attack of the rib to the main stream flow. The effect of each of these parameters will be discussed separately.

Rib height-to-hydraulic diameter

Ribs of rectangular cross-section were machined onto the plate surface at 90° to the direction of main stream flow. The pitch to height ratio was kept

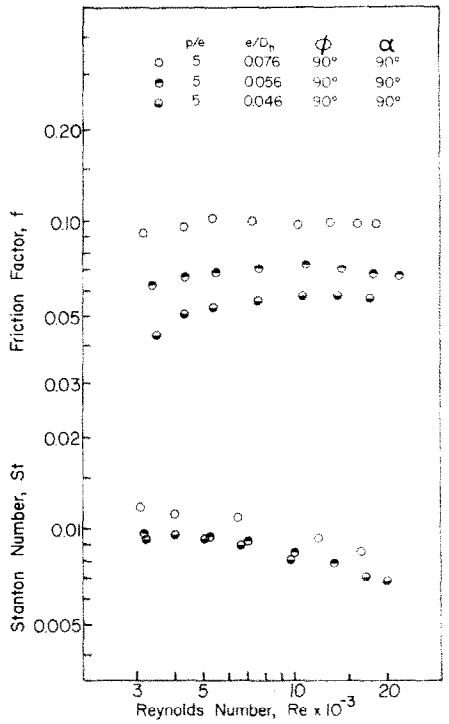

FIG. 6. Friction factor and Stanton number vs Reynolds number for different e/D_h ratios.

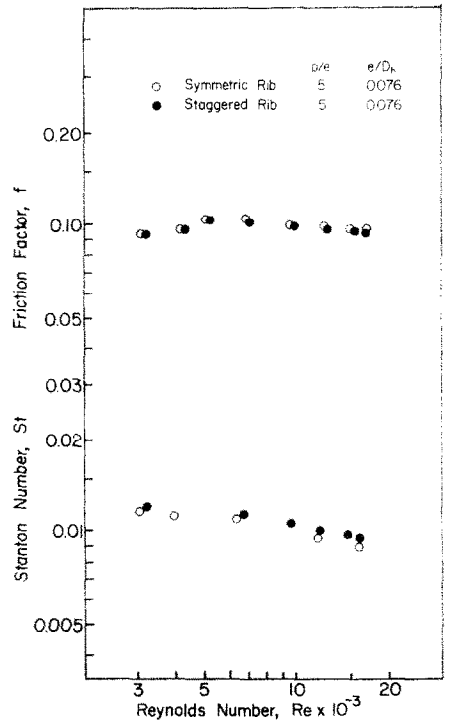

FIG. 7. Friction factor and Stanton number for symmetric and staggered ribs.

constant for this series of tests. The friction factor and Stanton number derived from the test results are shown on Fig. 6. Since the ribs are made of a high conductivity material they are at the same temperature as the plate. All calculations of the Stanton number are based on the total transfer surface area including the rib surface area. At a given ratio of the rib height to

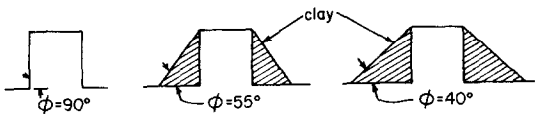

FIG. 8. Model of rib shapes.

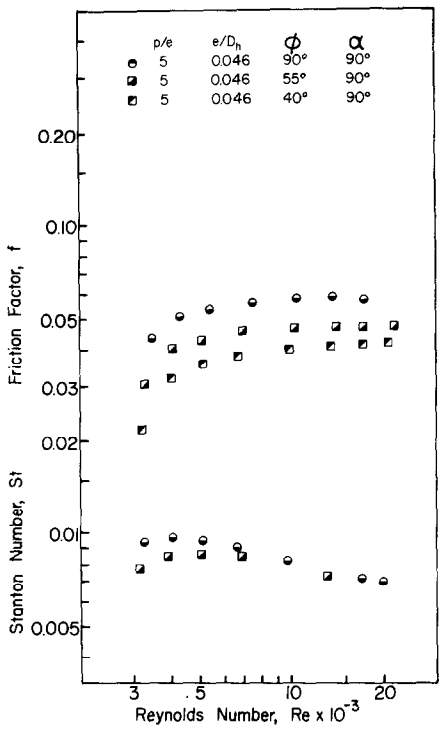

FIG. 9. Friction factor and Stanton number for different rib shapes.

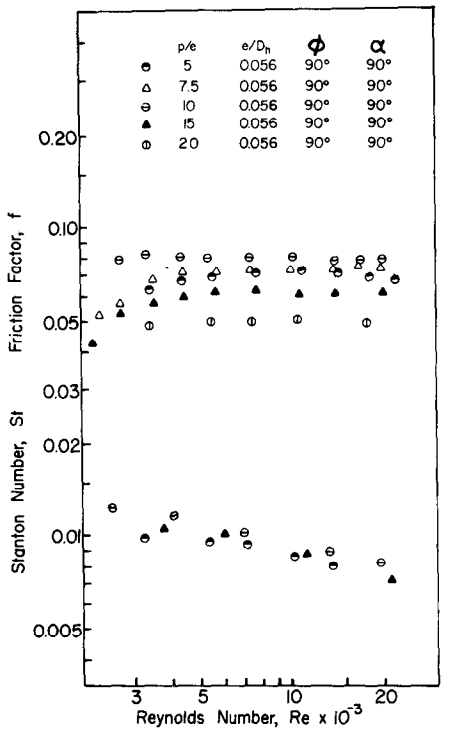

FIG. 10. Friction factor and Stanton number for different p/e ratios.

hydraulic diameter, e/D_H, the friction factor approaches a constant value as the Reynolds number increases; whereas the Stanton number continues to decrease with Reynolds number. As e/D_H increases, the friction factor increases. For the test results in Fig. 6, the two plates were symmetrical. In Fig. 7, test results for staggered plates are compared with the symmetrical test results. Figure 1 illustrates the staggered geometry which was tested. Although the rib height is approximately 15% of the plate separation distance, the alignment of the rib has a very modest effect on the friction factor and on the Stanton number.

Rib cross-section

Figure 8 shows the cross-section of the ribs which were used in the test. Modeling clay was used to fill in the corners of the rectangular ribs to create two distinct geometries shown on the figure. When the angle ϕ is 40°, resistance of the clay will reduce the local heat-transfer rate by about 20%. For this reason the latter geometry was not used in the heat-transfer tests. For ϕ of 55°, the thermal resistance of the clay reduces the heat flux by approximately 8% for the area covered by the clay. For the entire surface, the error in the average heat-transfer coefficient due to the thermal resistance of the clay is approximately 4%. In Fig. 9 it is seen that as corners of the ribs are filled in, the friction factor decreases. The clay has a much more modest effect on the heat-transfer coefficient. The influence of the rib shape on the Stanton number disappears at higher Reynolds number where the flow is in the completely rough regime.

Rib pitch

Five different values of the rib pitch-to-height ratio were tested. These ribs are manufactured by either machining a small section off the top of the rib or by glueing additional ribs to the plate surface. For a glue thickness of five thousands of an inch or less, the heat-transfer flux to the portion of the plate under the rib is reduced by less than 3%; thus the thermal resistance of the glue is negligible. It has been found in the literature that small changes to the rib cross-section from square to rectangular should have a negligible effect on the friction factor and the heat transfer [18]. As P/e increases from its lowest value, the friction factor and the heat transfer also increases, Fig. 10. The maximum value of both of these quantities occur at a P/e of about ten. Notice that the friction factor increases slowly with P/e ratios less than 10, whereas for values of P/e greater than 10, the friction factor falls quite dramatically. Experimental results may be explained qualitatively from the flow behavior over the ribs. For small rib pitch-to-height ratios, e.g. P/e equal to five, the flow which separates after each rib does not reattach before it reaches the succeeding rib. At a P/e value of about 10, the flow does reattach close to the next rib. For larger rib spacings the reattachment point is reached and a boundary layer begins to grow before the succeeding

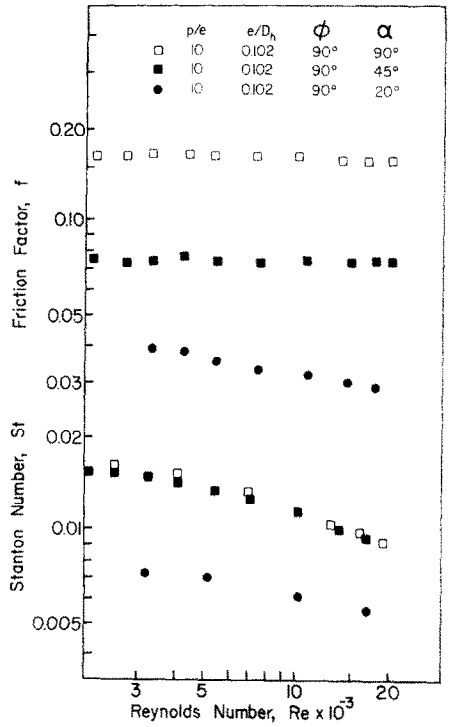

FIG. 11. Friction factor and Stanton number vs Re for different flow attack angles.

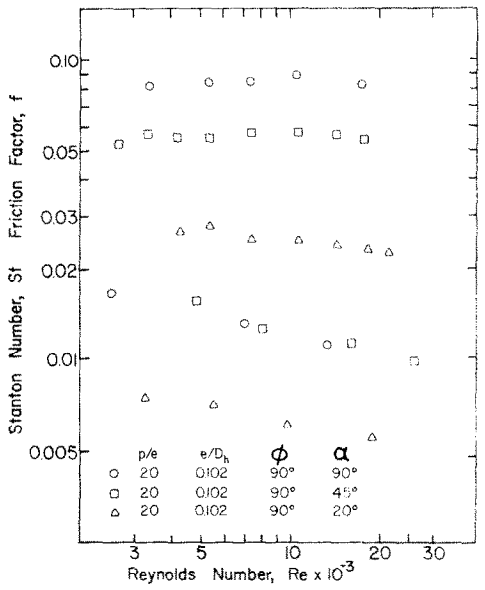

FIG. 12. Friction factor and Stanton number vs Reynolds number for different flow attack angles.

rib is encountered, reducing both the average shear stress and heat transfer.

Flow attack angle

Measurements were made for four different angles of attack, α, between the ribs and the main stream flow: 90°, 75°, 45°, and 20°, respectively. The pitch in this case is measured in the flow direction. For the two P/e ratios tested, the friction factor falls quite rapidly as the angle of attack decreases, see Figs. 11 and 12. However,

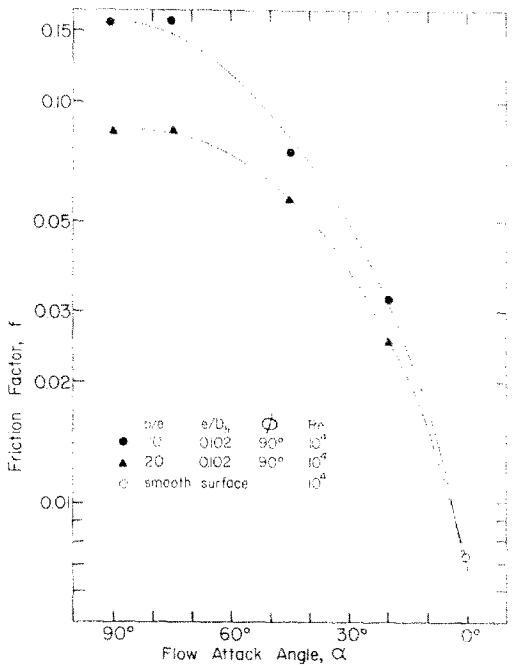

FIG. 13. Friction factor vs flow attack angles.

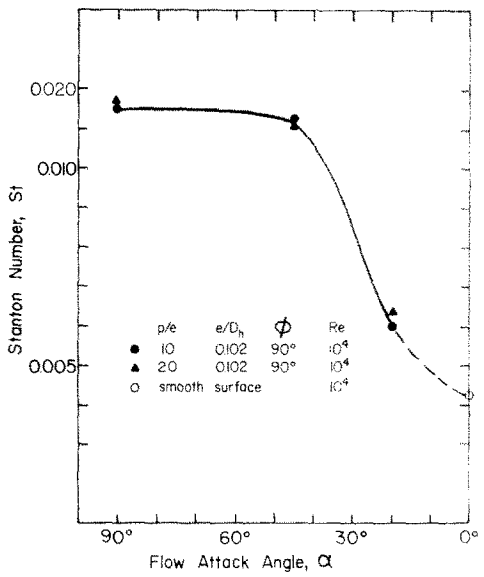

FIG. 14. Stanton number vs flow attack angles.

as the angle of attack changes from 90° to 45°, the Stanton number only decreases by 5%. Figures 13 and 14 show the variation of friction factor and Stanton number respectively with flow attack angle for a Reynolds number of 10^4. Values for the smooth surface are also indicated on these diagrams. For clarity, only a single value of Reynolds number is used in the figure; however, examination of Figs. 11 and 12 reveals that the same trend of friction factor and Stanton number with flow attack angle occurs over the entire range of Reynolds numbers tested. These results indicate that an attack angle near 45° represents the optimum thermal-hydraulic performance.

The friction factor decreases with angle of attack

because the form drag, which makes no contribution to the heat transfer, is being reduced. The rib still has a capability at a 45° flow angle of breaking up the laminar sublayer and enhancing the heat transfer. As the angle of attack is decreased further, both the heat transfer and the friction approach the smooth wall case.

V. FRICTION FACTOR CORRELATION

For the results of roughened surfaces to be most useful, general correlations are necessary for both the friction factor and the heat-transfer coefficient which cover a wide range of parameters.

In fully developed turbulent flow, theoretical approaches to the problem of momentum transfer in smooth and rough tubes have been available for many years. These approaches are based on similarity considerations. Two surfaces are said to have geometrically similar roughness if the geometry of their roughness is the same in all aspects except for a scale factor. For example, sand grain roughness is a geometrically similar roughness. With repeated-rib roughness, for a given flow attack angle, rib shape and pitch-to-height ratio, tests with a different height-to-hydraulic diameter ratio represent geometrically similar roughness. However, when the values of P/e, flow attack angle or rib cross-section are varied, the surfaces are not geometrically similar. Surfaces which are not geometrically similar will require modifications to the roughness and heat transfer functions found by similarity considerations.

Considering first friction factors for geometrically similar roughness, the basic assumptions used are the velocity defect law and the law of the wall similarity. The first of these implies, for turbulent flow in a channel, the existence of a region, away from the immediate vicinity of the wall, where the direct effect of viscosity and roughness on the core flow is negligible. This velocity defect law is described by equation (3), where the constant was proposed by Prandtl.

$$(U_c - U)/U^* = 2.5 \ln(R/y). \tag{3}$$

The law of the wall implies the existence of a region close to the wall where the velocity distribution depends on the local conditions, y, ρ, ν, τ and e. The law of the wall similarity is described by equation (4).

$$U/U^* = \psi[y/e, eU^*/\nu] = \psi[y/e, e^+]. \tag{4}$$

Assuming a region of overlap, the velocity defect law and the law of the wall similarity are combined to give equation (5) for the turbulence dominated part of the wall region with Re^+ a function of e^+.

$$U/U^* = 2.5 \ln(y/e) + Re^+(e^+). \tag{5}$$

Based on these analyses, Nikuradse developed the friction similarity law for sand-grain roughness surface by assuming equation (5) holds approximately over the entire cross-section. His data, covering a wide range of e/D_h, was correlated by equation (6), where e^+ is the roughness Reynolds number $[e^+ = e/D_h Re(f/2)^{1/2}]$.

$$Re^+(e^+) = (2/f)^{1/2} + 2.5 \ln(2e/D_h) + 3.75. \tag{6}$$

Equation (6) is the so-called friction similarity law. The roughness function Re^+ is a general function determined empirically for each type of geometrically similar roughness. The roughness function for Nikuradse's sand-grain roughness has the constant value 8.48 when e^+ is greater than 70; i.e. in completely rough regime, Re^+ does not depend on e^+. However, it is expected to be different for different geometrical roughness configurations. Based on the "friction similarity law", Webb *et al.* [10] found a successful friction correlation for turbulent tube flow with repeated-rib roughness by taking into account the geometrically non-similar roughness parameter, the p/e ratio. That was

$$Re^+(e^+) = 0.95(P/e)^{0.53} \text{ for } P/e \geqslant 10,\ e^+ \geqslant 35. \tag{7}$$

This concept can be extended to correlate the friction data for turbulent flow between parallel plates with repeated-rib roughness by taking into account the geometrically non-similar roughness parameters of p/e, rib shape (ϕ), and flow attack angle (α). Figure 15 shows the roughness function vs roughness Reynolds number for a geometrically similar roughness, varying the ratio e/D_H using the present data. e/D_H was varied by changing the plate spacing. The hydraulic diameter was defined using only the roughened surface of the channel; i.e. assuming the channel walls were infinite parallel plates. While neglecting the side walls can cause an error of between 4–8% when all the channel walls are smooth; when the plates are rough neglecting the smooth side walls should have a much smaller effect on the results. This is seen in Fig. 15 where

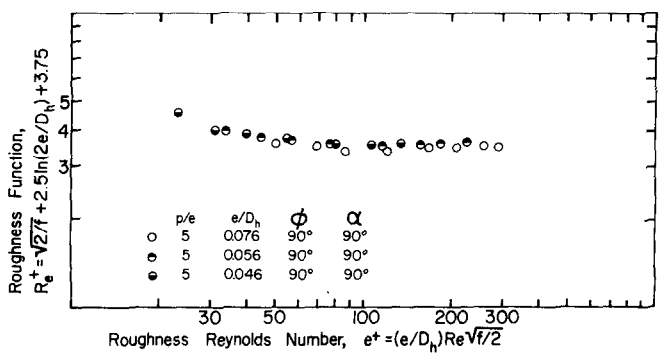

FIG. 15. Roughness function vs roughness Reynolds numbers for different e/D_h ratios.

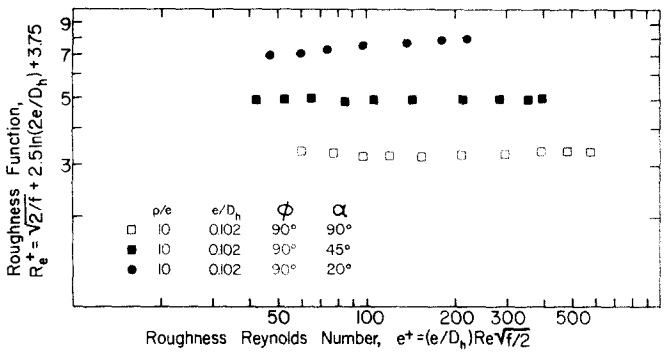

FIG. 16. Roughness function vs roughness Reynolds number for different flow attack angles.

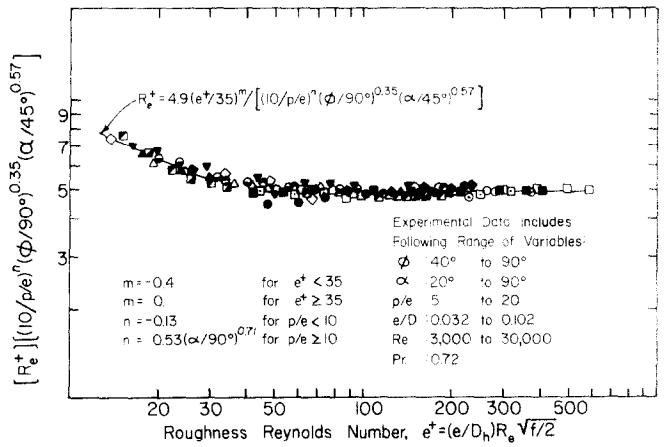

FIG. 17. Final friction correlation.

variations in e/D_H cause a negligible change in Re^+. Figure 16 shows the roughness function for a non-similar roughness, varying the angle of attack. The data of Figs. 15 and 16 along with data for variation of P/e and rib cross-section can be correlated into a single curve. This relationship, shown in Fig. 17, is

$$Re^+ = 4.9(e^+/35)^m/[(\phi/90°)^{0.35}(10/P/e)^n(\alpha/45)^{0.57}] \quad (8)$$

where

$$m = -0.4 \text{ if } e^+ < 35;$$
$$m = 0 \text{ if } e^+ \geq 35$$
$$n = -0.13 \text{ if } P/e < 10;$$
$$n = 0.53(\alpha/90°)^{0.71} \text{ if } P/e \geq 10.$$

The friction factor can be found by combining equations (6) and (8).

Equation (8) is the general correlation for the friction factor measured for eleven different dissimilar rib-type geometries and sixteen different geometries in all. When the roughness Reynolds number is 35 or larger the flow is in the completely rough regime. The form of the equation changes at P/e of 10. This roughly corresponds to the rib spacing necessary for the boundary layer to reattach to the plate. The approximate range of validity of the expression is given on Fig. 17. Since it was impossible to measure all combinations of the geometric parameters at the limits of this range, it is difficult to estimate a maximum uncertainty for the expression.

Friction data of other investigators

As mentioned before, many investigators have examined the effect of the e/D_h and P/e ratios on the friction factor and heat-transfer coefficient with a 90° flow attack angle and sharp-edged repeated-ribs (rectangular or square cross section). This is a special case of the general correlation given by equation (8) with ϕ and α equal to 90°. In order to compare this data with the other investigators' friction data, only the completely roughened regime will be considered. Equation (8) then becomes for ϕ and α equal to 90°.

$$Re^+ = 0.97(P/e)^{0.53} \text{ for } P/e \geq 10, \ e^+ \geq 35$$
$$= 4.45(P/e)^{-0.13} \text{ for } P/e \leq 10, \ e^+ \leq 35. \quad (9)$$

This is identical to Webb's expression, equation (7), with the constant changed from 0.97 to 0.95. Figure 18 shows a comparison of present data (for clarity only data for $P/e \leq 10$ is shown) with Webb's correlation, the data of Gargaud and Paumard [7] and Wilkie [11]. Wilkie took data for concentric tubes with the inside tube surface heated and roughened and the outside tube surface isothermal and smooth. Then using a simplification of the Hall transformation, the data was recalculated to apply to the case where both tubes have a roughened surface. Wilkie's data shows a

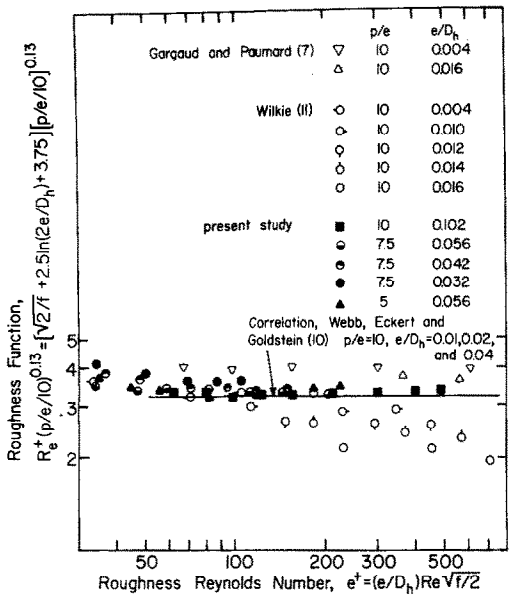

FIG. 18. Comparison of experimental data for different height-to-hydraulic diameter ratios for $P/e \leq 10$.

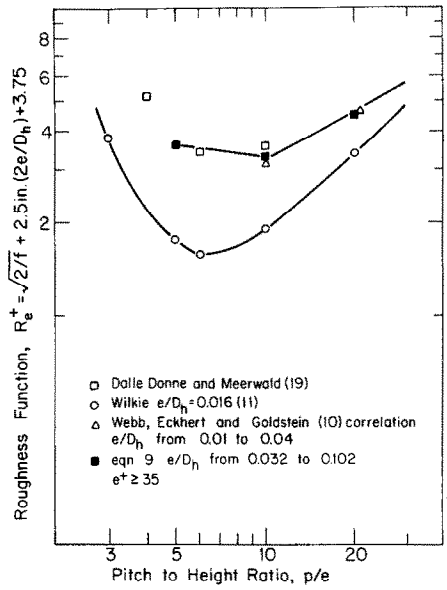

FIG. 19. Comparison of experimental data for different pitch to height ratios.

definite decrease in Re^+ with e^+ not evident in other data. This is possibly due to errors introduced through the use of Wilkie's transformation.

Dalle Donne and Meyer [15] present a correlation for Re^+ which includes a significant influence of the ratio of rib height, e, to the distance from the wall at which the surface of zero shear lies, $\hat{y}$. In the present experiment due to symmetry, $\hat{y}$ must be one-half the channel width. Thus, values of $e/\hat{y}$ range from 0.128 to 0.408 while for Webb's data, $e/\hat{y}$ is between 0.02 and 0.08. According to Dalle Donne and Meyer's correlation, Re^+ should increase as $e/\hat{y}$ varies from 0.01 to 0.235. At values of $e/\hat{y}$ greater than 0.235, Dalle Donne and Meyer claim that Re^+ should fall rapidly although no correlation is presented. The minimum value of $e/\hat{y}$ for Webb's data is 0.02; the maximum value of $e/\hat{y}$ for the present experiment which falls within Dalle Donne and Meyer's correlation is 0.224. By the correlation, at e^+ equal to 150, Re^+ should increase by 0.97 or 30% when $e/\hat{y}$ increases from 0.02 to 0.224. Comparing the present data with Webb's correlation it can be seen in Fig. 18 that the difference in the values of Re^+ are less than 6% and can be realistically assumed to be identical. When the average of all the data of the present experiment, represented in equation (8), is compared with Webb's correlation in the fully turbulent region, equation (9), the difference in Re^+ is 2%. Since neither of these experiments required a transformation to find Re^+, it seems probable that the influence of $e/\hat{y}$ on Re^+ found by Dalle Donne and Meyer is caused by their particular transformation. Therefore it is doubtful if $e/\hat{y}$ has any influence on Re^+ at least up to the maximum value of $e/\hat{y}$ examined in the current experiment.

Equation (9) is plotted in Fig. 19 along with data for P/e ratios from 5 to 20. The data of Webb *et al.* are also plotted in Fig. 9 for P/e of 10 and 20. It must be pointed

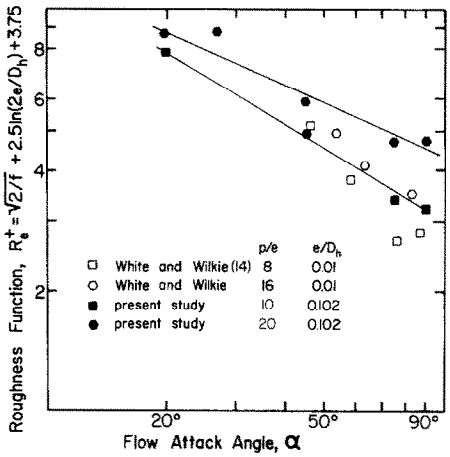

FIG. 20. Comparison of experimental data for different flow attack angles.

out that equations (7) and (9) represent many test data of different e/D_h ratios at the given P/e value. Dalle Donne and Meerwald have run experiments with sharp-edged square ribs for P/e less than 10, their results are given in a paper by Lewis [19]. Wilkie's data [11, 20] are also plotted on Fig. 19. It can be seen that the data of Webb *et al.*, and Dalle Donne and Meerwald agree quite well with this investigation, although Dalle Donne's data at very small ratios disagrees with the proposed correlation. Wilkie's data differs by 35% at a P/e of 10, by 20% at a P/e of 20, and by 50% at a P/e of 5. The lack of agreement of Wilkie's data with that of other investigators indicates the inaccuracies inherent in the transformation he used. In the completely roughened regime and with sharp-edged ribs, equation (8) reduces to

$$Re^+ = 4.9(45°/\alpha)^{0.57}\left(\frac{P/e}{10}\right)^n. \qquad (10)$$

Equation (10) is plotted in Fig. 20 with P/e ratios of 10 and 20. White and Wilkie ran experiments for a P/e ratio of 8, and 16, and Reynolds number varying between 7.5×10^4 to 2×10^5. White and Wilkie's results were found by transforming data obtained for flow in annular tubes. At a flow attack angle of 75°, the two investigations have a 25% difference. The difference is most likely due to the errors inherent in the transformation method; it appears unlikely that White and Wilkie's ribs caused any appreciable helical flow in section. They assume that there are two regions: a roughness region near the wall ($0 \leqslant y \leqslant e$), and a fully turbulent core region ($e \leqslant y \leqslant y_0$). For the turbulent core region, assume $v \ll \varepsilon_m$, $\alpha \ll \varepsilon_h$, $\varepsilon_m \simeq \varepsilon_h$, $U = U_0$ and $T = T_m$ at $y = y_m$, and assume the linear distributions of shear stress and heat flux hold. In the roughness region, based on the law of the wall and friction similarity, the velocity distribution is a function of (y, ρ, ν, τ_0, e). Then based on the heat and momentum transfer analogy, the temperature distri-

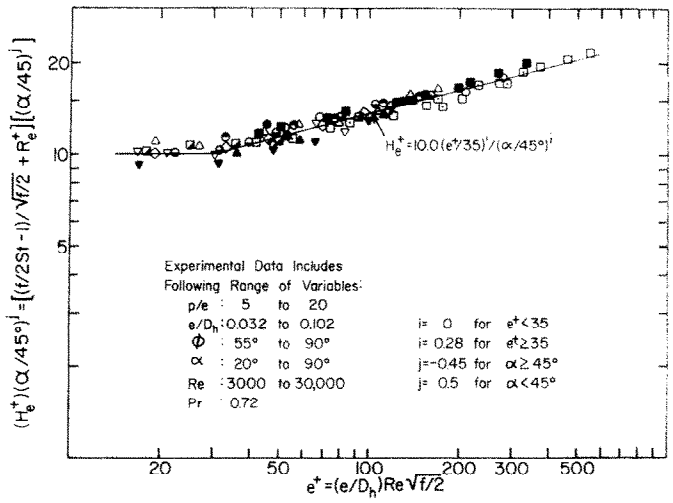

FIG. 21. Final heat-transfer correlation with Stanton number based on total area.

the channel due to the small value of e/D_h they used. No other data could be found which could be compared with the present work for varying angles of attack.

VI. HEAT TRANSFER CORRELATION

Consider the momentum equation in the y-direction of a steady, fully developed turbulent flow between parallel flat plates. The shear stress is balanced by the pressure drop, where the shear stress includes the molecular and turbulent shear stress. Since in fully developed flow the pressure gradient is uniform across the stream, τ_0 varies linearly with y. The momentum equation becomes

$$(\tau_0/\rho)(y - y/y_0) = (\nu + \varepsilon_m)(\mathrm{d}U/\mathrm{d}y). \quad (11)$$

Similarly consider the energy equation for a steady fully developed turbulent flow between parallel flat plates. The heat transfer into the fluid from the wall is equal to the temperature rise of the fluid. In fully developed flow with constant $\dot{q}/A$ at wall, one can approximately assume that the term $(\rho c_p u)(\partial T/\partial X)$ is constant, thus the apparent heat flux varies linearly with y. The energy equation can be written as,

$$(\dot{q}/A)_0(1 - y/y_0)/\rho c_p = -(\alpha + \varepsilon_H)(\mathrm{d}T/\mathrm{d}y). \quad (12)$$

Based on these analyses, Dipprey and Sabersky [21] developed the heat-transfer similarity law for sand-grain roughness surface by assuming equations (11) and (12) hold approximately over the entire cross-

bution between the rough wall and the distance y_m, can also be resolved into the same two regions. Dividing equation (11) by equation (12), and integrating the result from 0 to e, and from e to y_m, one gets equation (13).

$$\frac{f/(2St) - 1}{(f/2)^{1/2}} + Re^+ = \int_0^{e^+} \frac{(\nu + \varepsilon_m)}{\alpha + \varepsilon} \frac{\mathrm{d}U^+}{\mathrm{d}y^+} \mathrm{d}y^+. \quad (13)$$

For given values of f and Re^+, the rough surface Stanton number can be computed if the RHS of equation (13) is known. This requires a quantitative understanding of the details of the flow over the surfaces. However, if the integrand in equation (13) can be defined as functions of known variables, the equation will define the parameters necessary to correlate the rough surface heat-transfer data. From equation (5), U/U^* or U^+, is a function of e^+, and assuming that ε_m and ε_h are functions of e^+ and $\mathrm{d}U^+/\mathrm{d}y^+$, equation (13) may be rewritten as,

$$\frac{f/(2St) - 1}{(f/2)^{1/2}} + Re^+ = He^+(e^+, Pr). \quad (14)$$

If He^+, Re^+, and the friction factor are known, then the Stanton number can be found as,

$$St = \frac{f}{[He^+ - Re^+](2f)^{1/2} + 2}. \quad (15)$$

Equation (14) is the "heat transfer similarity law". He^+ is the heat-transfer function. It should be re-emphasized that both functions Re^+ and He^+ depend

on the specified type of geometrically similar roughness. For example, Dipprey and Sabersky found experimentally that He^+ equals $5.19(e^+)^{0.2}(Pr)^{0.44}$ for sand-grain roughness in turbulent tube flow. Based on the "heat transfer similarity law", Webb *et al.* found a successful heat transfer similarity relationship for turbulent flow with repeated-rib roughness by taking into account the geometrically non-similar geometry.

$$He^+ = 4.5(e^+)^{0.28}(Pr)^{0.57} \tag{16}$$

Webb's experimental data indicated that the effect of pitch to height ratio on He^+ is small for P/e ratios between 10 and 40, so P/e does not appear explicitly in equation (16).

This concept has been extended to correlate the friction data for turbulent flow between parallel plates with repeated-rib roughness by taking into account the geometrically non-similar roughness parameters of P/e, rib shape, and flow attack angle of the present investigation. The final heat-transfer correlation, shown in Fig. 22, is

$$He^+ = 10(e^+/35)^i/[\alpha/45°]^j$$

where

$$i = 0 \text{ when } e^+ < 35;\ i = 0.28 \text{ when } e^+ \geqslant 35$$
$$j = 0.5 \text{ when } \alpha < 45°;\ j = -0.45 \text{ when } \alpha \geqslant 45°. \tag{17}$$

For the correlation St is based on the total heat-transfer area. Note that the experiments have shown that He^+ is not a function of ϕ or P/e. To approximately take into account the Prandtl number effect, He^+ in equation (17) may be replaced by $(He^+)(0.72/Pr)^{0.57}$. This is taken from Webb's experimental data where the Prandtl number was varied from 0.72 to 37.6.

White and Wilkie [14] also found a trend of He^+ with α similar to that given by equation (17). However, their values of He^+ were 25% or more below those found in this study. A more complete derivation of the friction and heat-transfer correlation presented in this paper can be found in [22].

Comparison of heat-transfer data

There are two methods of calculating the heat-transfer coefficient of rib-roughened surfaces. First, the heat-transfer coefficient can be based on the projected area of the heat-transfer surface; alternatively, the heat-transfer coefficient can be based on the total area of the heat-transfer surface, i.e. including the rib area. When P/e is large, this effect is small. However for a small value of P/e the ribs constitute an appreciable fraction of the total area. Since metallic ribs of approximately square cross-section are used in this study they attain a temperature close to that of the plate. For this reason, the correlations for the heat-transfer coefficient are based upon the total area.

Most investigations based the heat-transfer coefficient on the projected surface area rather than the total area. For purposes of comparison, the data is replotted in Fig. 22 with the Stanton number based on the projected area. The agreement of the data with Webb's correlation is seen to be quite good. When St is based on the projected area, equation (17) becomes,

$$He^+ = 8(e^+/35)^i/[\alpha/45°]^j \tag{18}$$

where i and j have the same values as in equation (17).

In practice, the choice of the particular equation to use, either based on total area or projected area depends on the rib construction. If the rib is a tall thin strip made of low conductivity material the latter should be used. However, when the rib is a thick high conductivity material, found, for example, when the rib is formed by stamping the plate, the former is preferred. Equation (18) was also compared with White and Wilkie's data. For an e^+ of 130, White and Wilkie's data differed by 30% at a flow attack angle of 77°, by 20% at a flow attack angle of 45°, and by 40% at a flow attack angle of 27°. As mentioned before, the discrepancy may be due to errors in the transformation they used.

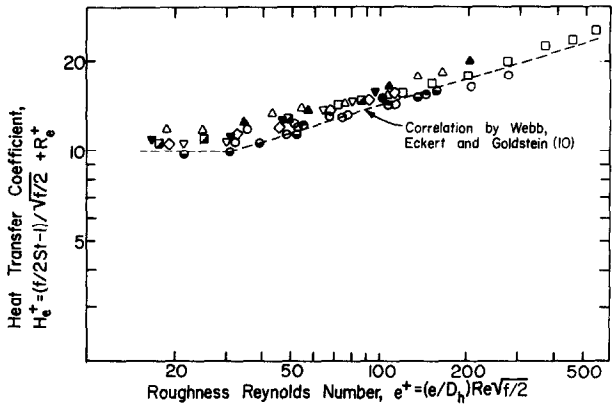

FIG. 22. Comparison of present data with Webb's correlation, St based on projected area.

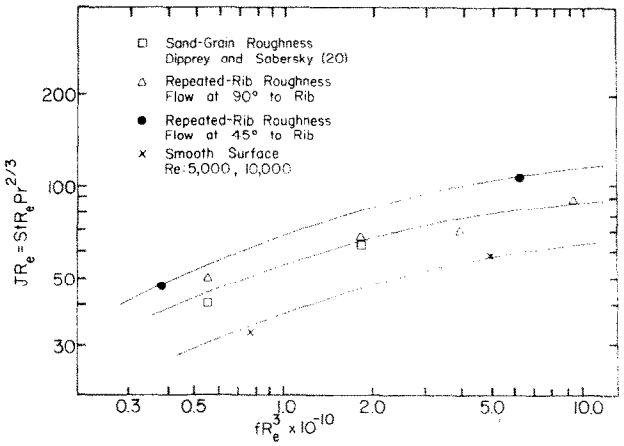

FIG. 23. Performance comparison.

VII. PERFORMANCE COMPARISON

Mack and Rohsenow suggested a method to compare the performance of the different types of roughened surface [23]. In Fig. 23, the horizontal axis is proportional to the pumping power per unit heat exchanger volume. The vertical axis represents the NTU, $hAs/\dot{m}c_p$ per unit volume for the same fluid at the same temperature levels. Fluid properties are

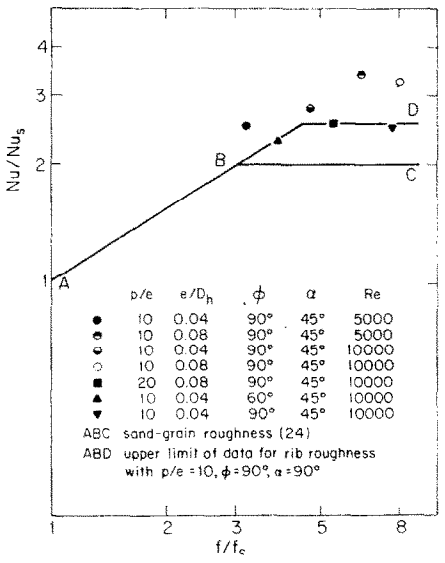

FIG. 24. Performance of different types of rib roughness.

assumed constant; and the hydraulic diameter is the same for the surfaces being compared. For a given pumping power per unit volume, the repeated-rib of this investigation with a 45°flow attack angle has a higher heat transfer per unit volume than sand-grain roughness or repeated ribs with a 90° flow angle.

A comparison of different types of roughened surfaces can also be made using the form suggested by Norris [24]. In this form, the Nusselt number is compared to the friction factor with each referenced to corresponding quantities for a smooth surface. Plotting the results in the form suggested by Norris also eliminates the question of the correct Prandtl number dependence for various kinds of rough surfaces. The results are shown on Fig. 24 with the upper limits for sand-grain roughness and for ribs normal to the flow compared to data for ribs at a 45° angle to the flow direction.

VIII. CONCLUSIONS

Experimental results for rib roughened surfaces have been taken for parallel plates which do not rely on a transformation for data reduction. For flow between parallel rib roughened plates, a symmetrical arrangement of the plates gives approximately the same results as a staggered arrangement. Changing the rib cross-section has a marked effect on the friction factor and a very modest effect on the heat transfer. Both the Stanton number and friction factor have a maximum value when the pitch-to-height ratios of the rib is approximately ten.

Based on the law of the wall similarity and the application of a heat-momentum transfer analogy, general friction and heat-transfer correlations have been obtained by taking into account the effect of geometrically non-similar parameters.

Friction and heat-transfer correlations agree well with other investigators, although discrepancies are evident when the correlations are compared to data reduced by use of the Hall type transformation.

A performance comparison shows that the repeated-rib roughness with a 45° flow attack angle gives higher heat transfer for the same friction power than repeated-rib roughness with a 90° flow attack angle or sand-grain roughness.

Acknowledgement---This work was sponsored by the Empire State Electric Energy Research Corporation. Their support is gratefully acknowledged.

REFERENCES

1. J. Nikuradse, Laws for flow in rough pipes, NACA TM 1292 (1950).
2. W. F. Cope, The friction and heat-transfer coefficients of rough pipes, *Proc. Inst. Mech. Engrs* **145**, 99–105 (1941).

3. W. Nunner, Heat transfer and pressure drop in rough tubes, AERE Lib/Trans. 786 (1958).
4. E. W. Sams, Experimental investigation of average heat transfer and friction coefficients for air flowing circular pipes having square-thread type roughness, NACA RM-E 52-D17 (1952).
5. E. D. Brouillette, T. L. Mefflin and J. E. Myers, Heat transfer and pressure drop characteristics at internal finned tubes, ASME paper 57-A-47 (December 1957).
6. R. Koch, Pressure loss and heat transfer for turbulent flow, English Translation, AEC-Tr-3875 (1960).
7. J. Gargaud and G. Paumard, Ameloration du transfert de chaleur par emploi de surfaces corrugees, Commissariat a L'energy Atomique, Report CEA-R 2464 (1969).
8. J. Molloy, Rough tube friction factors and heat-transfer coefficients in laminar and transition flow, UKAEA AERE-R5415 (1967).
9. E. K. Kalinin, G. A. Dreistler and S. A. Yarkho, in *Augmentation of Convective Heat and Mass Transfer*, edited by A. E. Bergles and R. L. Webb. ASME, New York (1970).
10. R. L. Webb, E. R. G. Eckert and R. J. Goldstein, Heat transfer and friction in tubes with repeated-rib roughness, *Int. J. Heat Mass Transfer* **14**, 601–617 (1971).
11. D. Wilkie, Forced convection heat transfer from surfaces roughened by transverse ribs, in *Proceedings of the 3rd International Heat Transfer Conference*, Vol. 1. A.I.Ch.E., New York (1966).
12. N. Sheriff and P. Gumley, Heat transfer and friction properties of surfaces with discrete roughness, *Int. J. Heat Mass Transfer* **9**, 1297–1320 (1966).
13. W. B. Hall, Heat transfer in channels having rough and smooth surfaces, *J. Mech. Engng Sci.* **4**, 287–291 (1962).
14. L. White and D. Wilkie, The heat transfer and pressure loss characteristics of some multi-start ribbed surfaces, in *Augmentation of Convection Heat and Mass Transfer*, edited by A. E. Bergles and R. L. Webb. ASME, New York (1970).
15. M. D. Dalle Donne and L. Meyer, Turbulent convective heat transfer from rough surfaces with two-dimensional rectangular ribs, *Int. J. Heat Mass Transfer* **20**, 582–620 (1977).
16. W. M. Rohsenow and H. Y. Choi, *Heat, Mass and Momentum Transfer*. Prentice-Hall, Englewood Cliffs (1961).
17. J. P. Hartnett, J. C. Y. Koh and S. T. McComas, *J. Heat Transfer* **84**, 82 (1962).
18. F. Williams, M. A. M. Pirie and C. Warburton, Heat transfer from surfaces roughened by ribs, in *Augmentation of Convective Heat and Mass Transfer*, edited by A. E. Bergles and R. L. Webb. ASME, New York (1970).
19. M. J. Lewis, An elementary analysis for predicting the momentum and heat transfer characteristics of a hydraulically rough surface, *J. Heat Transfer* **97**, 299 (1975).
20. W. M. Rohsenow and J. P. Hartnett (editors), *Handbook of Heat Transfer*, pp. 7–47, 48. McGraw-Hill, New York.
21. D. F. Dipprey and R. H. Sabersky, Heat and momentum transfer in smooth and rough tubes at various Prandtl number, *Int. J. Heat Mass Transfer* **6**, 329–353 (1963).
22. Je-Chin Han, Convective heat transfer augmentation in channels using repeated-rib roughness, Sc.D. Thesis, Dept. of Mech. Engng, M.I.T. (September 1976).
23. W. M. Mack and W. M. Rohsenow, Evaluation of the heat transfer performance of three enhanced surfaces including an enhanced surface heat exchanger performance comparison method, Report No. DSR 74590-86, Heat Transfer Lab., Dept. of Mech. Engng (June 1974).
24. R. H. Norris, Some simple approximate heat transfer correlations for turbulent flow in ducts with rough surfaces, in *Augmentation of Convective Heat and Mass Transfer*, edited by A. E. Bergles and R. L. Webb. ASME, New York (1970).

ETUDE DU TRANSFERT THERMIQUE ET DU FROTTEMENT POUR DES SURFACES RUGUEUSES COTELEES

Résumé—Une étude de surface rugueuse est menée pour déterminer les effets de la forme des côtes, de l'angle d'attaque, du rapport du pas à la hauteur, sur le coefficient de frottement et sur le transfert thermique. Une géométrie à plaque parallèle est utilisée. Pour tenir compte de la forme de la côte, de l'espacement et de l'angle d'attaque, une relation générale pour le coefficient de frottement et le transfert thermique est proposée en se basant sur la loi de similitude de paroi et sur l'application de l'analogie de la quantité de mouvement développée par Dipprey et Sabersky. On trouve que les côtes avec un angle d'attaque de 45° ont des performances supérieures, pour une puissance de frottement donnée, à celles attaquées à 90° ou en comparaison de la rugosité granulaire.

EINE UNTERSUCHUNG VON WÄRMEÜBERTRAGUNG UND DRUCKVERLUST AN OBERFLÄCHEN MIT RIPPENFÖRMIGER RAUHIGKEIT

Zusammenfassung—Es wurde eine Untersuchung an einer rauhen Oberfläche mit Rippenstruktur durchgeführt, um die Auswirkungen der Rippenform, des Anströmwinkels und des Abstands-Höhen-Verhältnisses auf den Widerstandsbeiwert und den Märmeübergang zu bestimmen. Als geometrische Anordnung wurden parallele Platten gewählt. Unter Verwendung der von Dipprey und Sabersky entwickelten Analogie zwischen Wärme- und Impulsaustaustausch wurde eine allgemeine Korrelation zwischen Widerstandsbeiwert und Wärmeübergang formuliert, in welcher Rippenform, Teilung und Anströmwinkel berücksichtigt werden. Es ergab sich, daß Rippen mit einem Anströmwinkel von 45° bei gegebenem Strömungswiderstand im Vergleich zu Rippen mit 90° Anströmwinkel oder im Vergleich mit sand-rauhen Oberflächen bessere Wärmeübertragungseigenschaften haben.

ИССЛЕДОВАНИЕ ТЕПЛООБМЕНА И ТРЕНИЯ НА ОРЕБРЕННЫХ ПОВЕРХНОСТЯХ

Аннотация — Исследовалась оребренная поверхность для определения влияния формы ребра, угла атаки и отношения шага ребра к высоте на коэффициенты трения и теплообмена. Используя закон подобия стенки и аналогию между переносом тепла и количества движения, разработанную Диппри и Саберским, получено общее соотношение для коэффициентов трения и теплообмена, учитывающее форму ребра, расстояние между ребрами и угол атаки. Найдено, что ребра с углом атаки в 45° обладают более высокой тепловой эффективностью при той же величине трения, чем ребра с углом атаки в 90° или поверхность с зернистой шероховатостью.